1. Introduction

Atypical benign partial epilepsy in childhood (ABPE) initially presents with the following signs and symptoms: (i) onset age of 2.5–6 years; (ii) multiple seizure types including focal motor, atypical absences and myoclonic-atonic seizures; (iii) electroencephalography (EEG) showing central and mid-temporal spikes and diffuse slow spike-wave activities during drowsiness or sleep; and (iv) normal development or mild mental retardation [1]. Despite multiple seizure types and slow spike and waves on EEG, ABPE is distinguished from Lennox–Gastaut syndrome by its characteristic spontaneous remission, lack of tonic seizures or developmental delay, and normal awake EEG background activity. Since hemi-convulsive seizures during sleep and contralateral/bilateral centro-temporal epileptiform discharges are present at the beginning, the electro-clinical findings of ABPE are indistinguishable from those of benign epilepsy with centro-temporal spikes (BECTS) [2–5]. BECTS is the most well-recognized, age-related idiopathic focal epilepsy with occasional epileptic seizures despite frequent centro-temporal spikes on EEG. In contrast, ABPE patients tend to develop atypical absences or myoclonic-atonic seizures during the course of their condition. Tovia et al. [6] showed that 0.5% of patients with BECTS were categorized as atypical variants, while Doose et al. [7] found that 29% of the relatives of ABPE patients had some abnormal activities on EEG. Finally, Gobbi et al. [8] reviewed several subtypes of idiopathic focal epilepsies to categorize ABPE as a "Rolandic epilepsy-related disorder"; these age-related epilepsies including ABPE and BECTS were attributed to a maturational continuum with different manifestations.

Epileptic negative myoclonus (ENM) is one of the characteristic seizure patterns in ABPE. Oguni et al. [6] analyzed the ictal EEG findings of ENM and demonstrated generalized, bilateral synchronous discharges, while ictal magnetoencephalography (MEG) of an ABPE patient showed that the spike sources of ENM were localized at the peri-sylvian region [7].

MEG is a relatively new clinical technique that uses superconducting quantum interference devices (SQUIDs) to measure and localize sources of extracranial magnetic fields generated by intraneuronal electric currents. Current MEG machines have a whole-head array of more than 100 sensors contained within a helmet-shaped Dewar, which effectively covers most of the brain surface. MEG has been increasingly used for localization of the epileptic zone and functional mapping in epilepsy patients. MEG in BECTS patients showed spike sources with an anterior–posterior oriented perpendicular to the Rolandic fissure [8,9]. No case series of ABPE have thus far used MEG to localize epileptic spike sources.

We conducted a multi-center study to collect clinical, EEG and MEG findings in ABPE patients, with MEG used to characterize the spike sources (MEGSSs) in ABPE. We hypothesize that the epileptic network in ABPE is localized in both the Rolandic-sylvian cortex and thalamo-cortical networks, based on their unique clinical and electrophysiological features.

2. Patients and methods

We collaborated with four institutions on this study: the Department of Pediatrics, Hokkaido University School of Medicine (HU); Department of Pediatrics, Tohoku University School of Medicine (TU); Department of Pediatrics, National Center of Neurology and Psychiatry (NCNP), Japan; and the Division of Neurology, The Hospital for Sick Children (HSC), Toronto, Ontario, Canada.

2.1. Patients

We studied 18 patients with ABPE (nine females and nine males). We diagnosed ABPE according to the triad of diagnostic criteria as follows: (1) focal motor seizures, absences/atypical absences, atonic seizures including ENM, myoclonic seizures and drop attacks described by parents; (2) EEG findings of central and middle temporal spikes and generalized slow spike-wave activity during drowsiness or sleep similar to continuous spike and slow waves during sleep (CSWS); (3) normal development or mild mental retardation during the clinical course.

2.2. EEG

Scalp video EEGs were recorded using the international 10-20 electrode placement system and electromyography (EMG) electrodes for bilateral deltoid muscles to capture ENM. Awake and sleep EEGs were recorded in all patients.

2.3. MEG and magnetic resonance imaging

Initial MEG studies were conducted at the onset of ENM. Seven patients had multiple MEG studies up to six times. Parents or guardians of all patients provided written informed consent for the MEG studies. MEG and EEG were done in a magnetically shielded room. MEG was recorded using a system with 306 SQUIDs (Vectorview; Elekta-Neuromag Ltd., Helsinki, Finland) at HU, NCNP and TU, and with an Omega system (151 channels, VSM MedTech Ltd., Port Coquitlam, BC, Canada) at HSC. MEG data were recorded with a band pass filter of 0.03–133 Hz at HU, NCNP and TU, and of 1–208 Hz at HSC. Sampling frequency was 400 Hz at HU, 600 Hz at NCNP and TU, and 625 Hz at HSC. EEGs were recorded using the international 10-20 system, with additional electrocardiogram (ECG)

Please cite this article in press as: Shiraishi H et al. Magnetoencephalography localizing spike sources of atypical benign partial epilepsy. Brain Dev (2013), http://dx.doi.org/10.1016/j.braindev.2012.12.011

electrodes. MEG data were recorded for >1 h per patient, collecting data in 4-min blocks at HU, NCNP and TU. At HSC, MEG was recorded in 15 two-minute blocks for a total of 30 min [10]. Patients were lying in the supine position. Sedative agents were used for uncooperative patients. The relative position of the head and the MEG sensors were determined by attaching three small head-position indicator coils to the head. The positions of the coils were digitized and subsequently recorded by the MEG sensors for co-registration with 1.5 T (tesla)/3 T magnetic resonance image (MRI) with high-resolution sequences.

2.4. MEG source analysis

MEG data were digitally filtered using a band filter of 3–30 Hz at HU, NCNP and TU, or at 3–70 Hz at HSC for offline analysis. Segments containing abnormal paroxysms were selected manually. Individual spikes were analyzed to localize the spike source per spike using an equivalent current dipole (ECD) model or dynamic statistical parametric mapping (dSPM) [11,12].

3. Results

3.1. Seizure profiles (Table 1)

Seizure onsets ranged from 1.3 to 8.8 years with a median age of 2.9 years. The seizures started as focal motor seizures in 15 patients (83%) and absences/atypical absences in three patients (17%).

All patients except one patient had multiple types of seizures in their seizure histories. Drop attacks, in which the precise seizure type remains unknown, were most common (16 patients, 89%). One patient (Patient 17) presented with a history of only drop attack seizures. Focal motor seizures (16 patients, 89%), ENM (14 patients, 78%), absences/atypical absences (11 patients, 61%), myoclonic seizures (10 patients, 56%) and secondarily generalized tonic-clonic seizures (nine patients, 50%) were seen in more than half of the patients (Supplementary videos 1 and 2). Focal sensory seizures (six patients, 33%) and epileptic spasms (two patients, 11%) were also reported.

Table 1
Seizure profiles.

Seizure onset	1.3–8.8 years (median, 2.9 years)	
Initial seizures	Focal motor seizures	15 (83%)
	Absences/atypical absences	3 (17%)
Type of seizures in patient history	Drop attacks	16 (89%)
	Focal motor seizures	16 (89%)
	Epileptic negative myoclonus	14 (78%)
	Absences/atypical absences	11 (61%)
	Myoclonic seizures	10 (56%)
	Secondarily generalized tonic-clonic seizures	9 (50%)
	Focal sensory seizures	6 (33%)
	Epileptic spasms	2 (11%)

3.2. Past and family history

There was no past history of epilepsy before the seizure onset in any of the 18 patients, while three patients (17%) had a positive family history of febrile seizures.

3.3. Cognitive functions

Cognitive function was evaluated in 15 patients. All 15 patients had the evaluations while they presented with ENM. A developmental quotient results ranged from 54 to 85 in five patients. The full-scale intelligence quotient test (Wechsler Intelligence Scale for Children) results ranged from 53 to 103 in 10 patients.

3.4. MRI

No patient showed an abnormality on MRI.

3.5. EEG (Fig. 1)

EEG showed interictal centro-temporal spikes in all 18 patients. Continuous generalized and/or centro-temporal spike and waves during sleep were also noticed in all patients. When video EEG captured ENM, generalized high-amplitude spike or polyspikes, and waves were associated with a brief attenuation of EMG activities corresponding to muscle atonia in 12 patients (Supplementary video 1). Absences/atypical absences showed generalized and irregular spike and slow waves around 3 Hz on EEG in 16 patients (Supplementary video 2).

3.6. MEG (Fig. 2 and Table 2)

MEG localized MEGSSs over both Rolandic and sylvian fissures in eight patients, the peri-sylvian region alone in five patients, and the peri-Rolandic region alone in four patients. One patient had MEGSSs in the left parieto-occipital region, even though EEG showed left centro-temporal spikes (Patient 6). Most spike sources were oriented perpendicularly to either the Rolandic or sylvian fissure. The spike sources demonstrated identical orientations in 11 patients (61%). MEGSSs were located in bilateral hemispheres in 10 patients (56%) and in a

Please cite this article in press as: Shiraishi H et al. Magnetoencephalography localizing spike sources of atypical benign partial epilepsy. Brain Dev (2013), http://dx.doi.org/10.1016/j.braindev.2012.12.011

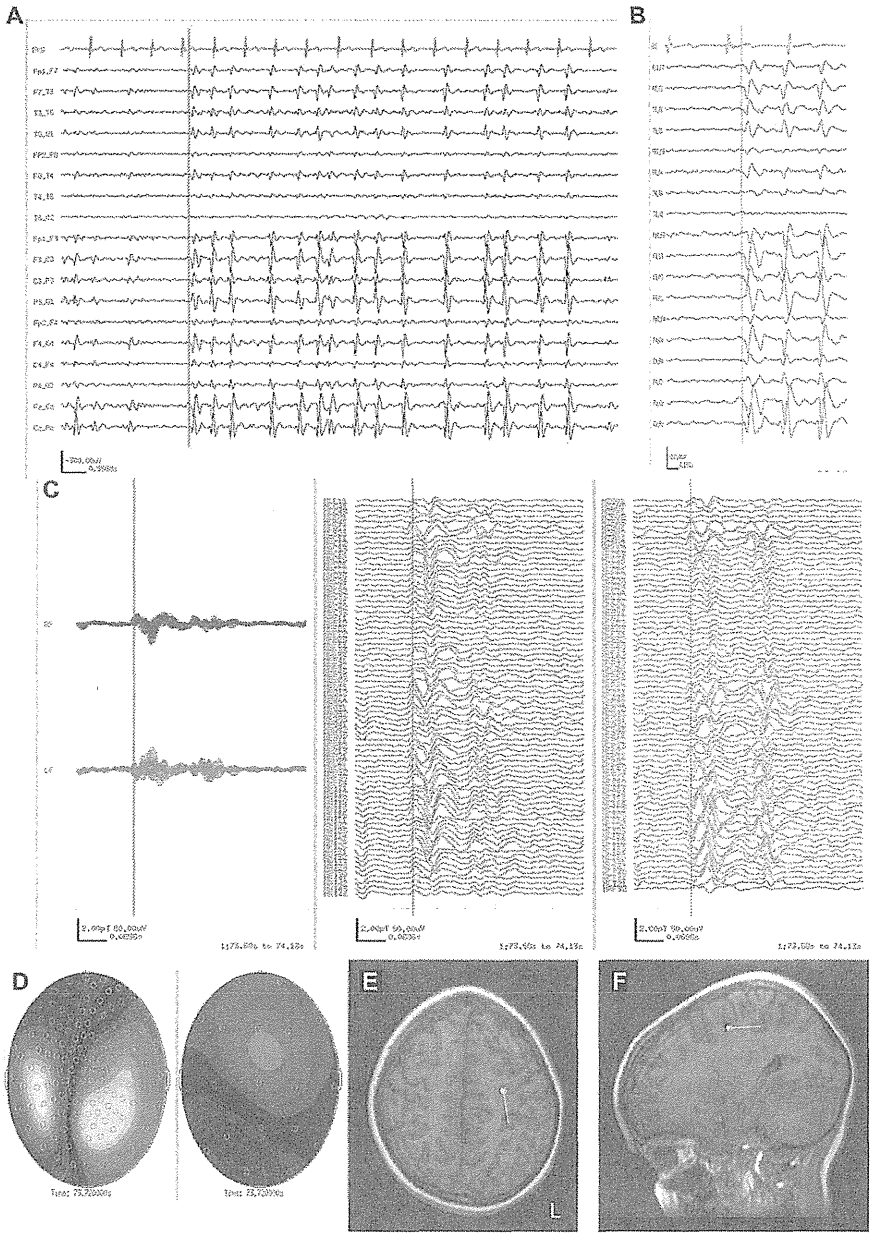

Fig. 1. MEG and EEG in case 18. (A) A–P bipolar EEG shows continuous spike and waves during sleep at the time of MEG study (low frequency filter, 3 Hz; high frequency filter, 70 Hz). (B) The same EEG of A is expanded to demonstrate left centro-temporal spikes preceding to the right central spikes after the red cursor. (C) 151 MEG channels are labeled by two colors (red for right hemisphere and blue for left hemisphere), and show the view of overlay (left), right channels (middle), and left channels (right). MEG shows more complex polyspikes than EEG on the overlay left channels. Note the MEG spikes (red cursor) leading to EEG spikes (behind the red cursor) on B. (D) MEG topography (left) and EEG topography (right). Note that magnetic and electric topographies are perpendicular to each other. (E) Axial MRI shows MEG spike source at the time of red cursor at the left Rolandic region (circle, position; tail, orientation, and moment). (F) Sagittal MRI shows the same MEG spike source of (E) at the left Rolandic region. The equivalent current dipole (spike source) is oriented horizontally, projecting negativity towards the frontal region and positivity towards the parietal region, corresponding to the EEG topography (D, right). (For interpretation of color in Fig. 1, the reader is referred to the web version of this article)

unilateral hemisphere in eight patients (44%). In all 10 patients with bilateral MEGSS, the MEGSS showed identical patterns and locations in the both hemispheres. ECD could not be estimated in one patient due to diffuse right hemispheric discharges without leading spikes. Therefore, we applied dSPM and localized the MEGSSs in the right sylvian fissure (Patient 7). Seven patients underwent multiple MEG studies. Six patients with

Please cite this article in press as: Shiraishi H et al. Magnetoencephalography localizing spike sources of atypical benign partial epilepsy. Brain Dev (2013), http://dx.doi.org/10.1016/j.braindev.2012.12.011

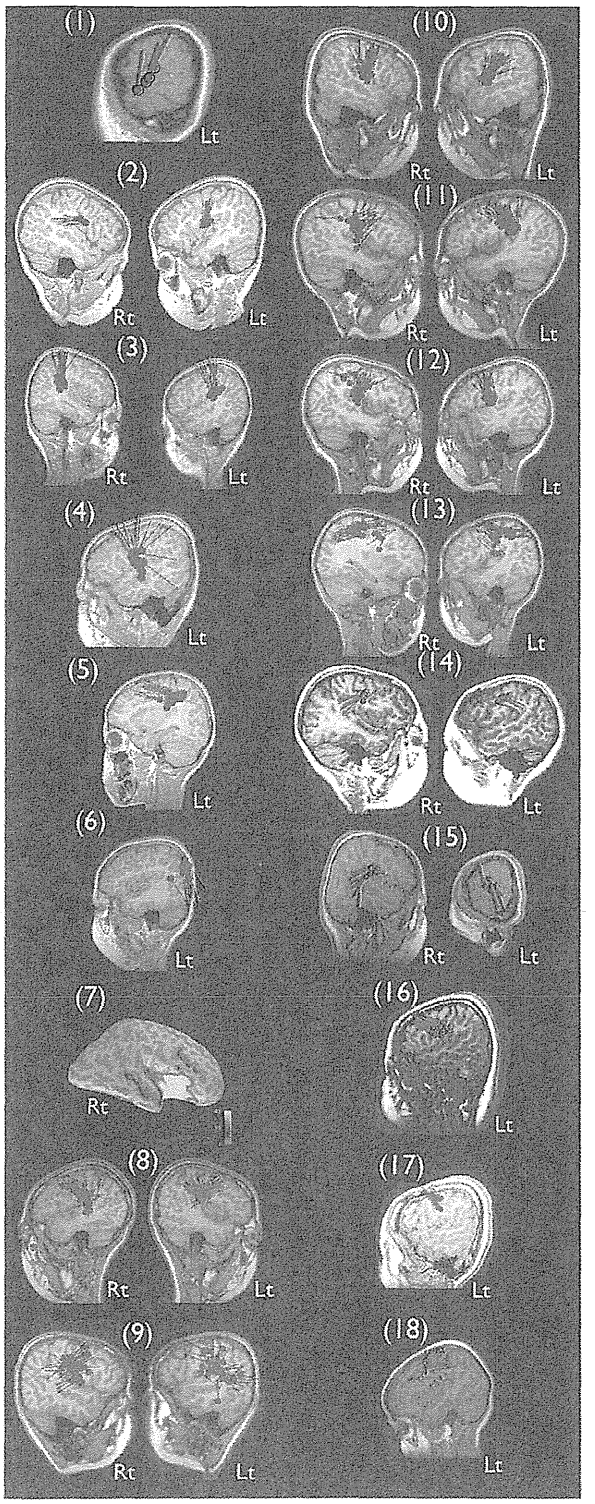

Fig. 2. MRI with MEG spike sources in 18 cases. Red circles demonstrate the source of MEG spikes. Tails indicate orientations and moments of the MEG spike sources. Case 7 shows dynamic statistical parametric mapping. The color bar indicates the *P* value, ranging from gray, 1×10^{-1} to yellow, $1 \times 10^{-4.3}$. (For interpretation of color in Fig. 1, the reader is referred to the web version of this article)

bilateral MEGSS became unilateral MEGSS. One patient showed consistent unilateral MEGSS. Six patients showed no MEGSS at the last MEG study when they were seizure free.

3.7. Treatments

All 18 patients were administered multiple antiepileptic medications ranging from 2 to 12 medications (mean 5.8) during their courses. Ethosuximide (ESM) succeeded in controlling various seizure types of ABPE, especially ENM and absences/atypical absences in 14 patients (78%); of these, all achieved seizure freedom after ESM was started, and 11 (89%) of the 14 were still on ESM at the last follow-up. Two of three patients in whom ESM was discontinued were no longer on any antiepileptic medication. CBZ was initially started in 16 patients (89%), but 14 (88%) experienced worsening of seizures after CBZ was initiated, and the treatment was discontinued. Two patients were seizure free on a combination of CBZ and ESM (Patient 6) or CBZ, ZNS and CLB (Patient 8). Valproic acid (VPA) was tried in 16 (89%) patients, and six of these (38%) were still on VPA at the last follow-up. Other medications tried included zonisamide (10 patients, 56%), clobazam (10 patients, 56%), clonazepam (eight patients, 44%) acetazolamide (five patients, 28%), phenytoin (five patients, 28%) and diazepam (four patients, 22%). The medications still being used at the last follow-up consisted of zonisamide in 3/10 patients (30%), clobazam in 4/10 patients (40%), clonazepam in 3/8 patients (38%), acetazolamide in 2/5 patients (40%) and diazepam in 2/4 patients (50%).

Two patients underwent epilepsy surgery. Patient 8 underwent cortical excision over the left supra-marginal gyrus at the age of 12 years. Surgical pathology revealed microdysgenesis with increased ganglion cells. She achieved 75–90% seizure reduction after the surgery, and was seizure free on three medications at 17.5 years old. Anterior two-thirds corpus callosotomy was performed at the age of 6 years for drop attacks in Patient 9. The patient was seizure free on two medications at 10 years old.

3.8. Seizure outcome

The age at last follow-up of the 18 patients ranged from 5.4 to 17.5 years (median 11.8 years). All were seizure free, two patients (11%) without any medication. Five patients (28%) were only on one medication, including four patients with ESM. The remaining 11 patients had multiple medications; six were on two medications, four were on three medications, and one patient was on four medications. Among seven patients with multiple MEG studies, medication changes, cognitive results effected less prominent for MEGSS than seizure improvements.

Please cite this article in press as: Shiraishi H et al. Magnetoencephalography localizing spike sources of atypical benign partial epilepsy. Brain Dev (2013), http://dx.doi.org/10.1016/j.braindev.2012.12.011

4. Discussion

MEG localized a Rolandic-sylvian epileptic focus of ABPE.

In ABPE, interictal MEG revealed localized clusters of spike sources around the Rolandic-sylvian fissures corresponding to both centro-temporal spikes and CSWS on EEG. The identically clustered Rolandic-sylvian MEGSSs of interictal epileptic discharges in patients with ABPE suggested that the epileptic focus was located around the Rolandic-sylvian regions involving the motor cortex in most cases. In our series, the peri-sylvian region MEGSSs were also recorded in 13 of 18 ABPE patients. In contrast, MEGSSs in BECTS were specifically localized along the Rolandic region with definite identical orientations vertical to the central sulcus [8,9]. In the older children with BECTS, MEGSSs shifted to the lower part of the Rolandic region close to the operculum.

Kubota et al. [10] reported an ictal MEG study localizing the spike source of ENM with generalized EEG spikes at the sylvian fissure in one ABPE patient [7]. ENM was characterized by spike or polyspikes on EEG time-locked to attenuation of EMG activity, which corresponded to muscle atonia [6]. Series of ENM often caused atonic seizures. Both interictal and ictal MEGSSs indicate that a subset of the epileptogenic zones responsible for focal seizures and ENM in ABPE patients is localized around the Rolandic-sylvian regions. In contrast, MEGSSs in three patients with Lennox–Gastaut syndrome with ENM were localized over inconsistent and various brain regions that did not include the Rolandic-sylvian regions [13].

Table 2
MEG spike source localization.

Patients	Regions			Hemispheres	
	Rolandic	Sylvian	Other lobe	Bilateral	Unilateral
1		1			1
2	1	1		1	
3		1		1	
4		1			1
5	1				1
6			Occipital		1
7		1			1
8	1	1		1	
9	1	1		1	
10		1		1	
11	1	1		1	
12	1	1		1	
13	1	1		1	
14	1			1	
15	1	1		1	
16	1				1
17	1				1
18	1	1			1
Total	12	13		10	8

Fifteen of eighteen patients in this series presented with focal motor seizures at the onset, and these persisted in addition to multiple other seizure types developing in 16 patients. ABPE might also be confused diagnostically with BECTS as ABPE appears superficially similar on scalp EEG and also presents with focal motor seizures. In ABPE patients, MEGSS extended to peri-sylvian region in addition to Rolandic region or localized even peri-sylvian region alone.

4.1. MEG localized spike dipoles in CSWS of ABPE

Sleep EEG often shows almost-continuous generalized or centro-temporal spike and waves during sleep in ABPE patients, resembling CSWS. Another differential diagnosis of ABPE is epileptic encephalopathy with CSWS (ECSWS), and there are no reports of source localizations using MEG in patients with ECSWS. The role of MEG remains to be explored in this entity. Kelemen et al. [17] reported three patients with CSWS secondary to destructive lesions in the thalamus [14], and CSWS development was often observed in patients with a thalamic lesion, indicative of thalamo-cortical dysfunction with an epileptic network [15,16]. ESM can be efficacious for seizures in ABPE patients, especially for ENM [6]. In 13 (72%) of the 18 ABPE patients studied herein, ESM completely suppressed their ENM. In other studies, systemic administration of ESM significantly reduced spike and wave discharges in genetic absence epilepsy models [17–19]. Continuous and generalized slow spike and waves during sleep in patients with ECSWS have been associated with secondary bilateral synchrony with leading foci [20,21]. The CSWS in ABPE could also be due to secondary bilateral synchrony, but originating specifically from the Rolandic-sylvian regions. The effect of ESM on the clinical seizures and CSWS indicates that the epileptic substitute of thalamic and Rolandic-sylvian networks produce ABPE.

Patry et al. [22] reported six patients with ECSWS, and heterogeneous seizure types of ECSWS that comprise focal motor seizures, absences, and epileptic falls while awake [21] resemble those of ABPE. Consequently, it can be difficult to distinguish ABPE from ECSWS clinically not analyzing the localization of epileptic foci. Further investigation of MEG in ECSWS may therefore serve to differentiate epileptic sources in these patients and improve our understanding of the epileptic networks and mechanisms leading to the observed cognitive disabilities.

5. Conclusions

MEG localized spike dipoles of centro-temporal spikes and CSWS over the Rolandic-sylvian regions in ABPE, indicating that ABPE is the localization-related

Please cite this article in press as: Shiraishi H et al. Magnetoencephalography localizing spike sources of atypical benign partial epilepsy. Brain Dev (2013), http://dx.doi.org/10.1016/j.braindev.2012.12.011

epilepsy with Rolandic-sylvian onset seizures. In addition, the effects of ESM on ENM and atypical absences suggest the involvement of thalamo-cortical circuitry in the epileptic network. ABPE is a unique age-related epilepsy involving the Rolandic-sylvian plus thalamo-cortical networks in the developing brain of children.

Disclosure of conflicts of interest

The authors have no financial or personal relations that could pose a conflict of interest.

Acknowledgment

We confirm that we have read the Journal's position on issues involved in ethical publication and affirm that this report is consistent with those guidelines.

Appendix A. Supplementary data

Supplementary data associated with this article can be found, in the online version, at http://dx.doi.org/10.1016/j.braindev.2012.12.011.

References

[1] Aicardi J, Chevrie JJ. Atypical benign partial epilepsy of childhood. Dev Med Child Neurol 1982;24:281–92.
[2] Beaumanoir A, Ballis T, Varfis G, Ansari K. Benign epilepsy of childhood with Rolandic spikes. A clinical, electroencephalographic, and telencephalographic study. Epilepsia 1974;15:301–15.
[3] Bernardina BD, Tassinari CA. EEG of a nocturnal seizure in a patient with "benign epilepsy of childhood with Rolandic spikes". Epilepsia 1975;16:497–501.
[4] Blom S, Heijbel J. Benign epilepsy of children with centro-temporal EEG foci. Discharge rate during sleep. Epilepsia 1975;16:133–40.
[5] Fejerman N, Caraballo R, Tenembaum SN. Atypical evolutions of benign localization-related epilepsies in children: are they predictable? Epilepsia 2000;41:380–90.
[6] Oguni H, Uehara T, Tanaka T, Sunahara M, Hara M, Osawa M. Dramatic effect of ethosuximide on epileptic negative myoclonus: implications for the neurophysiological mechanism. Neuropediatrics 1998;29:29–34.
[7] Kubota M, Nakura M, Hirose H, Kimura I, Sakakihara Y. A magnetoencephalographic study of negative myoclonus in a patient with atypical benign partial epilepsy. Seizure: J Br Epilepsy Assoc 2005;14:28–32.
[8] Minami T, Tasaki K, Yamamoto T, Gondo K, Yanai S, Ueda K. Magneto-encephalographical analysis of focal cortical heterotopia. Dev Med Child Neurol 1996;38:945–9.
[9] Ishitobi M, Nakasato N, Yamamoto K, Iinuma K. Opercular to interhemispheric source distribution of benign Rolandic spikes of childhood. NeuroImage 2005;25:417–23.
[10] RamachandranNair R, Otsubo H, Shroff MM, Ochi A, Weiss SK, Rutka JT, et al. MEG predicts outcome following surgery for intractable epilepsy in children with normal or nonfocal MRI findings. Epilepsia 2007;48:149–57.
[11] Dale AM, Liu AK, Fischl BR, Buckner RL, Belliveau JW, Lewine JD, et al. Dynamic statistical parametric mapping: combining fMRI and MEG for high-resolution imaging of cortical activity. Neuron 2000;26:55–67.
[12] Shiraishi H, Ahlfors SP, Stufflebeam SM, Takano K, Okajima M, Knake S, et al. Application of magnetoencephalography in epilepsy patients with widespread spike or slow-wave activity. Epilepsia 2005;46:1264–72.
[13] Sakurai K, Tanaka N, Kamada K, Takeuchi F, Takeda Y, Koyama T. Magnetoencephalographic studies of focal epileptic activity in three patients with epilepsy suggestive of Lennox–Gastaut syndrome. Epileptic Disord 2007;9:158–63.
[14] Kelemen A, Barsi P, Gyorsok Z, Sarac J, Szucs A, Halasz P. Thalamic lesion and epilepsy with generalized seizures, ESES and spike-wave paroxysms – report of three cases. Seizure: J Br Epilepsy Assoc 2006;15:454–8.
[15] Battaglia D, Veggiotti P, Lettori D, Tamburrini G, Tartaglione T, Graziano A, et al. Functional hemispherectomy in children with epilepsy and CSWS due to unilateral early brain injury including thalamus: sudden recovery of CSWS. Epilepsy Res 2009;87:290–8.
[16] Guzzetta F, Battaglia D, Veredice C, Donvito V, Pane M, Lettori D, et al. Early thalamic injury associated with epilepsy and continuous spike-wave during slow sleep. Epilepsia 2005;46:889–900.
[17] Hanaya R, Sasa M, Ujihara H, Fujita Y, Amano T, Matsubayashi H, et al. Effect of antiepileptic drugs on absence-like seizures in the tremor rat. Epilepsia 1995;36:938–42.
[18] Marescaux C, Micheletti G, Vergnes M, Depaulis A, Rumbach L, Warter JM. A model of chronic spontaneous petit mal-like seizures in the rat: comparison with pentylenetetrazol-induced seizures. Epilepsia 1984;25:326–31.
[19] van Rijn CM, Sun MS, Deckers CL, Edelbroek PM, Keyser A, Renier W, et al. Effects of the combination of valproate and ethosuximide on spike wave discharges in WAG/Rij rats. Epilepsy Res 2004;59:181–9.
[20] Kobayashi K, Nishibayashi N, Ohtsuka Y, Oka E, Ohtahara S. Epilepsy with electrical status epilepticus during slow sleep and secondary bilateral synchrony. Epilepsia 1994;35:1097–103.
[21] Tassinari CA, Rubboli G, Volpi L, Meletti S, D'Orsi G, Franca M, et al. Encephalopathy with electrical status epilepticus during slow sleep or ESES syndrome including the acquired aphasia. Clinical Neurophysiol 2000;111(Suppl. 2):S94–S102.
[22] Patry G, Lyagoubi S, Tassinari CA. Subclinical "electrical status epilepticus" induced by sleep in children. A clinical and electroencephalographic study of six cases. Arch Neurol 1971;24:242–52.

Please cite this article in press as: Shiraishi H et al. Magnetoencephalography localizing spike sources of atypical benign partial epilepsy. Brain Dev (2013), http://dx.doi.org/10.1016/j.braindev.2012.12.011

Epilepsy Research (2013) 104, 68–77

journal homepage: www.elsevier.com/locate/epilepsyres

Magnetoencephalographic analysis of paroxysmal fast activity in patients with epileptic spasms

Keitaro Sueda[a], Fumiya Takeuchi[b], Hideaki Shiraishi[a], Shingo Nakane[c], Kotaro Sakurai[d], Kazuyori Yagyu[a], Naoko Asahina[a], Shinobu Kohsaka[a], Shinji Saitoh[a,*]

[a] *Department of Pediatrics, Hokkaido University Graduate School of Medicine, Japan*
[b] *Department of Health Science, Hokkaido University School of Medicine, Japan*
[c] *Division of Magnetoencephalography, Hokkaido University Hospital, Japan*
[d] *Department of Psychiatry and Neurology, Hokkaido University Graduate School of Medicine, Japan*

Received 31 October 2011; received in revised form 28 August 2012; accepted 2 September 2012
Available online 5 October 2012

KEYWORDS
Magnetoencephalography;
Paroxysmal fast activity;
Epileptic spasms;
Lennox–Gastaut syndrome;
Time-frequency analysis;
Short-time Fourier transform

Summary
Purpose: This study sought to demonstrate the origin and propagation of paroxysmal fast activity (PFA) in patients with epileptic spasms (ESs), using time-frequency analyses of magnetoencephalogram (MEG) PFA recordings.
Methods: A 204-channel helmet-shaped MEG, with a 600 Hz sampling rate, was used to examine PFA in 3 children with ESs. We analyzed MEG recordings of PFA by short-time Fourier transform and the aberrant area or high-power spectrum was superimposed onto reconstructed three-dimensional magnetic resonance images as moving images. One ictal discharge was collected. One child and one adult with PFA due to Lennox–Gastaut syndrome were also examined for comparison.
Results: All four PFAs in Patient 1 and five PFAs in Patient 3 were generated from one hemisphere. In Patient 2, four of seven PFAs were generated from one hemisphere and the remaining three were generated from both hemispheres. In Patient 3, one ictal MEG showed ictal discharges that were generated from the same area as the PFA, although the electroencephalogram showed no discharge. In Patients with Lennox–Gastaut syndrome, all 10 PFAs were generated from bilateral hemispheres simultaneously.

* Corresponding author at: Department of Pediatrics, Hokkaido University School of Medicine, North15 West7, Kita-ku, Sapporo 060-8638, Japan. Tel.: +81 11 706 5954; fax: +81 11 706 7898.
E-mail address: ss11@med.nagoya-cu.ac.jp (S. Saitoh).

0920-1211/$ – see front matter
http://dx.doi.org/10.1016/j.eplepsyres.2012.09.001

Conclusion: Short-time Fourier transform analyses of MEG PFA can show the origin and form of propagation of PFA. These results suggest that ESs are representative of focal seizures and the mechanism of PFA is different between ESs and Lennox–Gastaut syndrome.

Introduction

Epileptic spasms (ESs) are seizures, with axial movements longer than myoclonus and shorter than tonic seizures, which occur either in clusters or periodically. Epileptic spasms have been identified in patients with diverse epilepsies (Ohtsuka et al., 2001; Gobbi et al., 1987). In the International League against Epilepsy (ILAE) Classification (1989), ESs are classified as focal, generalized, or unclear (Berg et al., 2010) and the mechanisms of ESs are unknown (Engel, 2006).

Fast activity is one of the characteristic patterns of an ictal electroencephalogram (EEG) in ESs (Watanabe et al., 2001). Paroxysmal fast activity (PFA) has been described by Brenner and Atkinson (1982), and is characterized by paroxysms of 1–9 s in duration, of high frequency (10–25 Hz) rhythmic activity, preceded or followed by generalized sharp and slow wave complexes. The paroxysms are widespread in distribution and bilaterally synchronous over both hemispheres, but may not always be generalized. Shifting asymmetries are common, but rarely the pattern may show persistent amplitude asymmetry and may be unilateral or even focal. PFA is seen most often in patients with Lennox–Gastaut syndrome (LGS), but is sometimes seen in patients with localized-related epilepsy, such as frontal lobe epilepsy or temporal lobe epilepsy (Markand, 2003).

Markand (2003) considered PFA to be a subclinical discharge. A magnetoencephalogram (MEG), which provides higher spatial and temporal resolution, may provide a method for analyzing PFA, which compensates for the deficiencies associated with EEG. The aim of this study is to describe the localization of MEG discharges corresponding to EEG PFA using short-time Fourier transform (STFT), a method of time-frequency analysis, in order to assess the mechanism of ESs.

Patients and methods

Patients

Three patients at Hokkaido University Hospital were enrolled in this study. The three patients had refractory ESs with multiple PFA on EEG. Two patients who had been diagnosed with LGS with multiple PFA were also enrolled in this study to compare the morphology and mechanism of each PFA. The clinical profiles of the five patients are summarized in Table 1. Tonic seizures, atypical absences and slow spike-waves, with cognitive deterioration were diagnostic of LGS (Arzimanoglou et al., 2009). All patients underwent magnetic resonance imaging (MRI), scalp ictal EEG, scalp interictal EEG and ^{99m}Tc L-ethyl cysteinate dimer single photon emission computerized tomography (^{99m}Tc-ECD-SPECT). The parents of all patients gave written informed consent for the study.

Patient 1
Patient 1 was a 6-year-old boy who had daily seizures. At 5 months of age, he began to have spasms with bilateral upper limbs contraction and head nodding. His EEG showed hypsarrhythmia and he was diagnosed with West syndrome. His MRI was normal. After adrenocorticotrophic hormone (ACTH) therapy, his seizures were resolved with valproate (VPA) and clobazam. At the age of 26 months, he began to have weekly seizures with sudden tonic posture of the extremities, complex partial seizures and spasms. His seizures were symmetric from clinical findings. His EEG showed bilateral central–parietal spikes. His seizures were refractory regardless of various antiepileptic drugs (AEDs): VPA, zonisamide (ZNS), phenytoin (PHT), carbamazepine (CBZ) and phenobarbital (PB). At the age of 36 months, interictal EEG showed Cz–Pz spikes and bilateral frontal spike and wave complexes. At the age of 50 months, interictal EEG showed PFA and bilateral Cz–Pz spikes. Ictal EEG showed fast rhythmic activity at the right central and left posterior temporal–occipital regions, followed by generalized spike and slow wave complexes. He had severe mental retardation. At the age of 6 years, he was referred to our hospital. He was diagnosed with symptomatic generalized epilepsy. Magnetic resonance imaging showed mild brain atrophy, while ^{99m}Tc-ECD-SPECT showed hypoperfusion bilaterally in the frontal lobes.

Patient 2
Patient 2 was a 10-year-old boy who had daily seizures. At the age of 5 months, he began to have spasms with bilateral upper limbs contraction and head nodding. His EEG showed hypsarrhythmia and he was diagnosed with West syndrome. After ACTH therapy, his seizures were initially resolved, but relapsed after 10 months. His spasms were symmetric from clinical findings. At the age of 3 years, asymmetric tonic seizures appeared which were refractory to various AEDs (VPA, PHT, ZNS, and CZP). He had severe mental retardation. At the age of 10 years, he was referred to our hospital. At this time, MRI showed mild brain atrophy. Interictal EEG showed PFA and bilateral diffuse polyspike and diffuse spike and wave complexes. Ictal EEG showed right central–parietal polyspikes and subsequent desynchronization. Bilateral hypoperfusion of the frontal lobes was shown by ^{99m}Tc-ECD-SPECT. He was diagnosed with frontal lobe epilepsy according to the neuroimaging and electro-clinical findings.

Patient 3
Patient 3 was a 19-year-old woman with daily seizures. At the age of 2 months, she began to have spasms with bilateral

Table 1 Patient profiles, MRI, EEG, interictal ECD SPECT findings.

	Age and sex	Sz onset	Sz type	Sz frequency	MRI findings	Interictal EEG	Ictal EEG	Interictal ECD SPECT	First diagnosis before MEG
Patient 1	6 y M	5 m	Epileptic spasms CPS Tonic posturing	Weekly	Brain atrophy	PFA Bil F SPW Bil C-P spikes	rt C. Lt pT polyspike →Diffuse spike	Bil F hypoperfusion	SGE
Patient 2	10 y M	5 m	Epileptic spasms Asymmetric tonic seizure Atypical absence	Daily	Brain atrophy	PFA Diffuse SPW	rt C-P polyspike →Desynchronization	Upside F hypoperfusion	FLE
Patient 3	19 y F	2 m	Epileptic spasms Myoclonic seizure Tonic posturing	Daily	NP	PFA Bil F dominant diffuse spikes and SPW	Desynchronization	Bil F-Tp hypoperfusion (L dominant)	SLRE (Undetermined localization)
Patient 4	14 y M	7 m	GT Atypical absence Astatic	Daily	Bil O gliosis	PFA Diffuse slow spike-waves	ND	Bil Tp-O hypoperfusion	Lennox–Gastaut syndrome
Patient 5	27 y F	11 y	Falling Atypical absence GT	Daily	Brain atrophy	PFA Diffuse slow spike-waves	Diffuse polyspike →Diffuse SPW	Bil Tp-O hypoperfusion	Lennox–Gastaut syndrome

Abbreviations: Sz, seizure; M, male; F, female; Lt, left; Rt, right; Bil, bilateral; ND, not done; SPW, spike and wave complex; NP, nothing particular; F, frontal; C, central; P, parietal; O, occipital; pT, posterior temporal; mT, mid temporal; SGE, symptomatic generalized epilepsy; FLE, frontal lobe epilepsy; SLRE, symptomatic localization related epilepsy; CPS, complex partial seizure; GT, generalized tonic seizure.

upper limbs contraction and head nodding and her EEG showed hypsarrhythmia. She was diagnosed as having West syndrome. After ACTH therapy, her seizures were initially resolved however they relapsed after a while. At the age of 2 years, she had tonic posturing of the upper limb and myoclonic seizures and her seizures were refractory to various AEDs (VPA, CBZ, CZP, PB, acetazolamide and nitrazepam) as well as ketogenic diets. At the age of 17 years, her seizures became ESs and tonic seizures. These seizures were symmetric from clinical findings, but her head deviated to left occasionally. Her interictal EEG showed PFA and bilateral frontal dominant diffuse spikes. Ictal EEG showed diffuse desynchronization in her ESs. At 19 years of age, ^{99m}Tc-ECD-SPECT showed hypoperfusion in the right frontal and temporal lobes dominantly. She was diagnosed with symptomatic localization-related epilepsy

Patient 4

Patient 4 was a 14-year-old boy with daily seizures. At 7 months of age, he had episodes of upper eye deviation with cyanosis and apnea. Phenobarbital and CBZ were administered because his EEG showed focal spikes and his seizures were resolved. At the age of 11 years, he had tonic seizures, drop attacks and atypical absences. Interictal EEG showed slow diffuse spike and waves and PFA, and he was diagnosed as having LGS. Magnetic resonance imaging showed gliosis bilaterally in the occipital and parietal lobes, and ^{99m}Tc-ECD-SPECT showed hypoperfusion in the area where the gliosis existed.

Patient 5

Patient 5 was a 27-year-old woman who had daily seizures. When she was 11 years old, she began to have weekly atypical absence seizures. Her seizures were refractory to various AEDs (VPA, CBZ, PHT, ZNS and clobazam). At the age of 15 years, she began to have tonic seizures with falling. She had mental retardation and was blind because of congenital cataracts. She was diagnosed with LGS. At the age of 27 years, MRI showed mild brain atrophy. Her EEG showed diffuse slow spike and wave complexes and PFA. Ictal EEG corresponding to her tonic seizures showed a diffuse fast rhythm and subsequent diffuse slow spike and wave complexes, while ^{99m}Tc-ECD-SPECT showed bilateral hypoperfusion of the temporal–occipital lobes.

Methods

Magnetoencephalogram recordings

Magnetoencephalograms were recorded by 204-channel helmet-shaped superconducting quantum interference devices (SQUIDs) (Neuromag Vectorview; Elekta-Neuromag, Co. Ltd., Stockholm, Sweden) with pairs of orthogonal planar gradiometers at 102 locations. The recordings were carried out in a magnetically shielded room. The patient lay in a supine position. The MEG data were collected for almost 40 min for each patient with a 600 Hz sampling rate. Scalp EEG was recorded simultaneously using the international 10–20 system with video monitoring. EMG at deltoid and ECG are recorded simultaneously. All patients took intravenous thiopental sodium for sedation to avoid motion artifact. Administration of thiopental sodium is routine and accepted procedure for sedation of child or handicapped patients in Hokkaido University Hospital.

Magnetoencephalogram data analysis

The MEG data were filtered for offline analysis with a band pass of 3–100 Hz. PFA is defined as assumption of rhythmic activity with four times heightened amplitude from background activity for more than 200 ms.The segments of MEG data that contained PFA were manually selected with one second in the vicinity of PFA to obtain whole PFA. The single dipole method (SDM) was used to try to analyze single spikes, to determine the distribution of the genesis of the spikes. PFA of MEG was analyzed by STFT to determine a specific frequency band and its localization.

Single dipole method

Dipole-fit software (Neuromag, Helsinki, Finland) was used to calculate the equivalent current dipoles (ECDs). We accepted significant ECDs with more than 70% of goodness of fit and between 100 and 800 nAm of dipole moment. Goodness of fit is a measure of how well the ECD model explains the measured signals. Acceptable ECDs were superimposed on the MRIs.

Short-time Fourier transform analysis

The STFT method was used to demonstrate the distribution of MEG rhythmic activities (**Oppenheim & Schafer, 1999**; **Sueda et al., 2010**). The MATLAB program (MathWorks, Natick, MA) was used to execute the STFT for the MEG signals. Each signal was divided into small sequential frames and fast Fourier transform applied to each frame.

In the present study, the STFT was implemented using a 256-point window. The time of each window was 426.7 ms (i.e., 256 points × 1000 ms/600 Hz). The window was shifted every four points which corresponded to 6.7 ms (i.e., 1000 ms/600 Hz × 4 points). Fast Fourier transform was applied to each window. This process was repeated for all the signals that were selected. The time–frequency distribution can be displayed as a graph as shown in **Fig. 1C**.

A spectrum was considered to be aberrant when it was observed in the graph to be isolated from the background frequency spectrum. An aberrant frequency spectrum on the graph was superimposed onto a reconstructed three-dimensional (3D)-MRI. The power spectrum of these aberrant frequency spectrums was located at the intersection of the line beneath the planer gradiometer coil and brain surface.

If there was a broadening of the frequency spectrum, the high-power spectrum, which could be seen as the red color on the graph, was selected. The high-power frequency spectrum was superimposed onto a reconstructed 3D-MRI. The location of the PFA origin was decided from the reconstructed 3D-MRI.

The time onset of the PFA in each hemisphere was decided when the oscillation emerged in the reconstructed 3D-MRI which could be seen in yellow or red area. The time

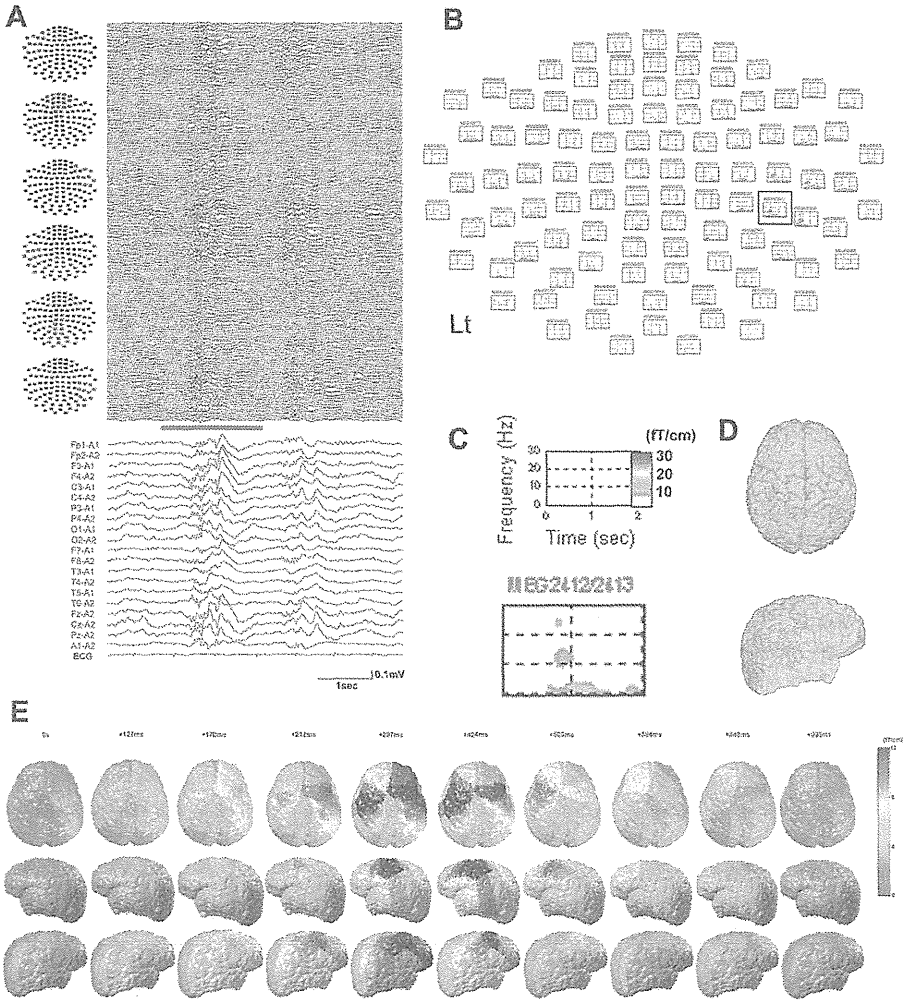

Fig. 1 (A) (Patient 1) Bottom panel demonstrates diffuse paroxysmal fast activity (PFA) of the electroencephalogram (EEG) and top panel shows the corresponding 204-channel magnetoencephalogram (MEG). (B) Short-time Fourier transform (STFT) graph of MEG PFA corresponding to the blue bar of (A). (C) Power spectrogram of MEG electrode 2412/2413 (black square in STFT graph B) using STFT to show the wide range of oscillations from 10 to 25 Hz. (D) Equivalent current dipoles are scattered bilaterally in the parietal region. (E) Specific oscillations at 10–25 Hz are generated in the right front–parietal area and propagated to the left front-parietal area in the superimposed three-dimensional magnetic resonance moving image of (B).

difference between PFA generation in each hemisphere was calculated using that time onset.

Magnetic resonance imaging

Magnetic resonance images were acquired with a 1.5 T high-resolution MRI scanner (Magnetom VISION, Siemens AG, Erlangen, Germany) for diagnostic purposes and co-registration with MEG data. Axial T1-weighted imaging (WI), T2–WI, fluid-attenuated inversion recovery (FLAIR), and coronal FLAIR sequences were performed.

Single photon emission computerized tomography

Interictal ^{99m}Tc-ECD-SPECT was performed for all patients. We used a ring-type SPECT scanner (Headtome-SET070; Shimadzu Corp., Kyoto, Japan).

Results

Table 2 summarizes the number of PFAs, pattern of PFA and origin of PFA for each patient with ESs. All four PFAs in Patient 1 and five PFAs in Patient 3 were generated from one hemisphere. For Patient 2, four out of seven PFAs were generated from one hemisphere and the remaining three were generated from both hemispheres simultaneously.

For patients with LGS (Patients 4 and 5), 10 PFAs were recorded, and all were generated from both hemispheres synchronously.

Patient 1

Four PFAs were captured during the recordings in Patient 1. Single dipole analysis was used for the spikes, but ECDs were not clustered. The results showed that his epileptiform

Table 2 Paroxysmal fast activity and Ictal EEG, MEG findings.

	Number	Pattern of EEG	Number	Origin in MEG	Number
Patient 1	4 PFA	PFA → PFA	2	rt F-P	2
		Single PFA	2	rt F-P	2
Patient 2	7 PFA	PFA → desyn→PFA	3	rt F-P	2
				bil F	1
		rt F-C spike → desyn→PFA	1	bil F	1
		Single PFA	2	rt F-P	2
		PFA → desyn	1	bil F	1
Patient 3	5 PFA	PFA → desyn → PFA	1	rt C-P	1
		PFA → desyn	2	rt F-C-T	1
				rt C-P-T	1
		Single PFA	2	rt F-C	1
				rt C-P-T	1
	1 ictal	No finding	1	rt C-P-T	1

Abbreviations: PFA, paroxysmal fast activity; desyn, desynchronization; rt, right; bil, bilateral; F, frontal lobe; C, central; P, parietal lobe; O, occipital lobe; T, temporal lobe.

discharges were not suitable for single dipole analysis (Fig. 1D). His MEG showed PFA corresponding to the EEG PFA in the bilateral frontal–parietal areas (Fig. 1A, top panel). Analysis using STFT showed a significant power spectrum in the range from 10 to 30 Hz (Fig. 1B and C). The 3D-MRI movie showed that all PFAs were generated in the right frontal–parietal lobe and propagated to the left frontal lobe discontinuously (Fig. 1E). The time differences of the PFA between the right and left hemisphere were 47–161 ms (mean, 129 ms).

Patient 2

Seven PFAs were captured during the recordings in Patient 2. Equivalent current dipoles were scattered throughout both hemispheres in the frontal-parietal lobes. The boy's MEG showed PFA corresponding to the EEG PFA bilaterally in the frontal area. Short-time Fourier transform analysis showed a significant power spectrum in the range from 10 to 30 Hz. The 3D-MRI movie showed that four of the seven PFAs were generated in the right frontal–parietal lobe and propagated to the left frontal lobe discontinuously. The time differences of the PFA between the right and left hemisphere were 73–149 ms (mean, 126 ms). However three PFAs were generated simultaneously from bilateral frontal lobes.

Patient 3

Five PFAs were captured during the recordings in Patient 3. Although ECDs were located in bilateral hemispheres, most ECDs were scattered in the right parietal area (Fig. 2E). The MEG showed PFA corresponding to the EEG PFA in the right central–parietal–temporal area (Fig. 2A, top panel). Analysis of PFA by STFT showed a significant power spectrum in the range from 10 to 25 Hz. The 3D-MRI moving image showed that PFA was generated in the right angular gyrus and propagated contiguously to the postcentral gyrus and superior parietal lobule (Fig. 2B).

Ictal EEG and MEG of ESs were obtained simultaneously (Fig. 2C). Short-time Fourier transform analysis before the onset of a clinical seizure showed a specific aberrant 10–18 Hz oscillation band, although the EEG showed no specific findings (Fig. 2C, shown in the blue line STFT 1). The 3D-MRI moving image showed that the specific oscillation band was generated in the right inferior parietal lobule (Fig. 2D). Analysis by STFT during the onset of a clinical seizure showed no specific aberrant oscillation (Fig. 2C, shown in the blue line STFT 2). The high-power area of the PFA was overlapped with the high-power area of the ictal paroxysmal discharge in the MEG.

Patient 4

Five PFAs were captured during the recordings in Patient 4. The ECDs were not clustered. The 204-channel MEG showed diffuse PFA in bilateral areas corresponding to the EEG PFA (Fig. 3A, top panel). The STFT analysis of the PFA showed that there was a wide range of PFA frequencies from 10 to 30 Hz (Fig. 3B). The power spectrogram of STFT showed constant high-power frequency at 10 Hz (shown in red on the power spectrogram in Fig. 3C). The 3D-MRI movie showed that all PFAs were generated simultaneously from bilateral hemispheres (Fig. 3D).

Patient 5

Five PFAs were captured during the recordings in Patient 5. The ECDs were not clustered. The 204-channel MEG showed diffuse PFA in bilateral areas corresponding to the EEG PFA (Fig. 3E, top panel). Short-time Fourier transform analysis of PFA showed that there was a wide range of PFA frequencies from 10 to 30 Hz, though the high-power frequency was 13–15 Hz (Fig. 3G). The 3D-MRI movie showed that all PFAs were generated simultaneously from both hemispheres (Fig. 3H).

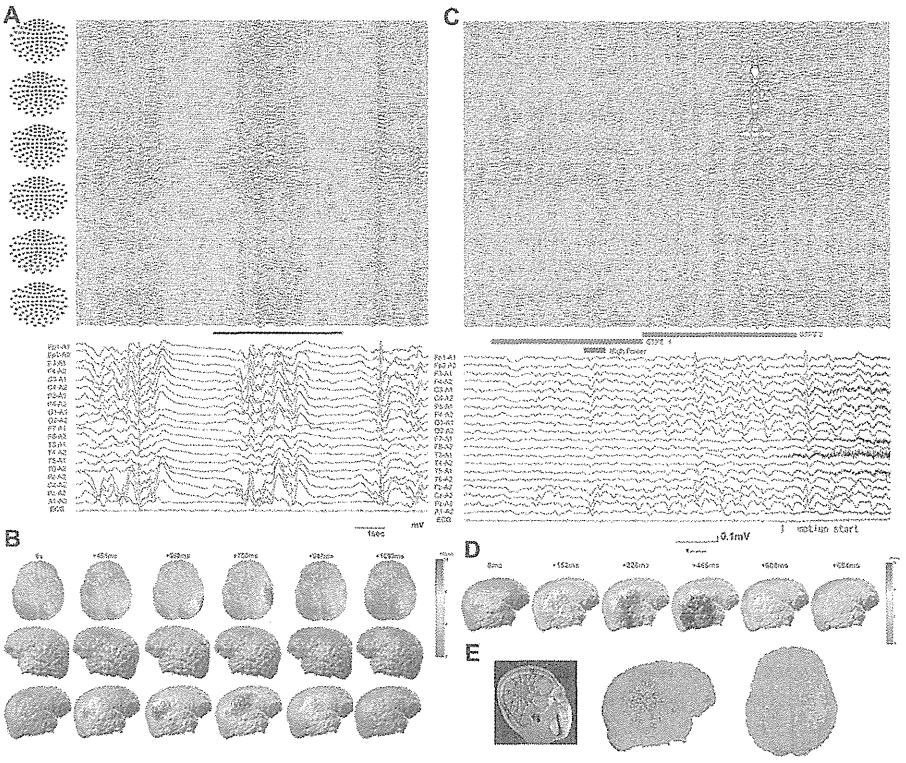

Figure 2 (A) (Patient 3) Bottom panel demonstrates interictal diffuse paroxysmal fast activity (PFA) of the electroencephalogram (EEG) with desynchronization before and after PFA, and top panel shows the corresponding 204-channel magnetoencephalogram (204ch-MEG). (B) Specific oscillations at 10—25 Hz are generated in the right parietal—temporal area in the superimposed three-dimensional magnetic resonance (3D-MRI) moving image. (C) Bottom panel demonstrates ictal EEG. Top panel shows the corresponding 204ch-MEG. Short-time Fourier transform graph shows specific oscillations in the right parietal—temporal area at the timing of the red bar. (D) Specific oscillations at 10—18 Hz are generated in the right parietal—temporal area in the 3D-MRI moving image. (E) Equivalent current dipoles are scattered in the right parietal region.

Discussion

In this study, we found that most of the PFA in patients with ESs was generated from a focal area of one hemisphere using STFT analysis of MEG data.

Recently several studies using different neuroimaging techniques, such as positron emission tomography (Chugani et al., 1994), SPECT (Munakata et al., 2004), and near-infrared spectrophotometry (Haginoya et al., 2002), have shown that focal areas play a role in the pathogenesis of ESs. Akiyama et al. (2005) reported that high frequency oscillations, recorded on digital video subdural EEG, were generated from the fronto-temporal region before and during clinical spasm and that focal cortical resection of the prominent area of high frequency oscillation eliminated the spasms. They suggested that ESs have the characteristics of partial seizures with secondary generalization. Panzica et al. (1999) reported that an asymmetric EEG pattern, mainly consisting of a rhythmic burst of fast activity, precedes both symmetric and asymmetric spasms. They suggested that a localized cortical origin of the ictal discharge gives rise to the spasms. In an electrocorticographic (ECoG) study, fast-wave burst activity was correlated with the clinical onset of spasms (Asano et al., 2005). RamachandranNair et al. (2008) reported that the sensory—motor cortex was part of the ictal-onset zone with ictal high-frequency oscillations in patients with ESs, and Asano and colleagues (2005) reported that ESs with fast-wave burst involvement of the sensory—motor cortex appeared to correlate with the severity of contralateral limb movements. Our MEG results support previous reports that a focal area plays a role in the pathogenesis of ESs.

All the patients were injected thiopental sodium intravenously. Thiopental constructs fast activity in the beta range (12—30 Hz). However, these fast activities are bilaterally symmetric and expanded in a frontal—central area, similar to those emerging during drowsiness (Feshchenko et al., 1997, 2004). The fast activity in Patients 1—3 were generated unilaterally. Those in Patients 4 and 5 were generated bilaterally symmetric, though not in a frontal—central area but in diffuse area. Therefore, the fast activity in our study was not attributed to thiopental.

Ictal and interictal PFA

We consider that analysis of interictal fast activity is equivalent to analysis of ictal fast rhythm, since all patients with ESs showed PFA which was followed by

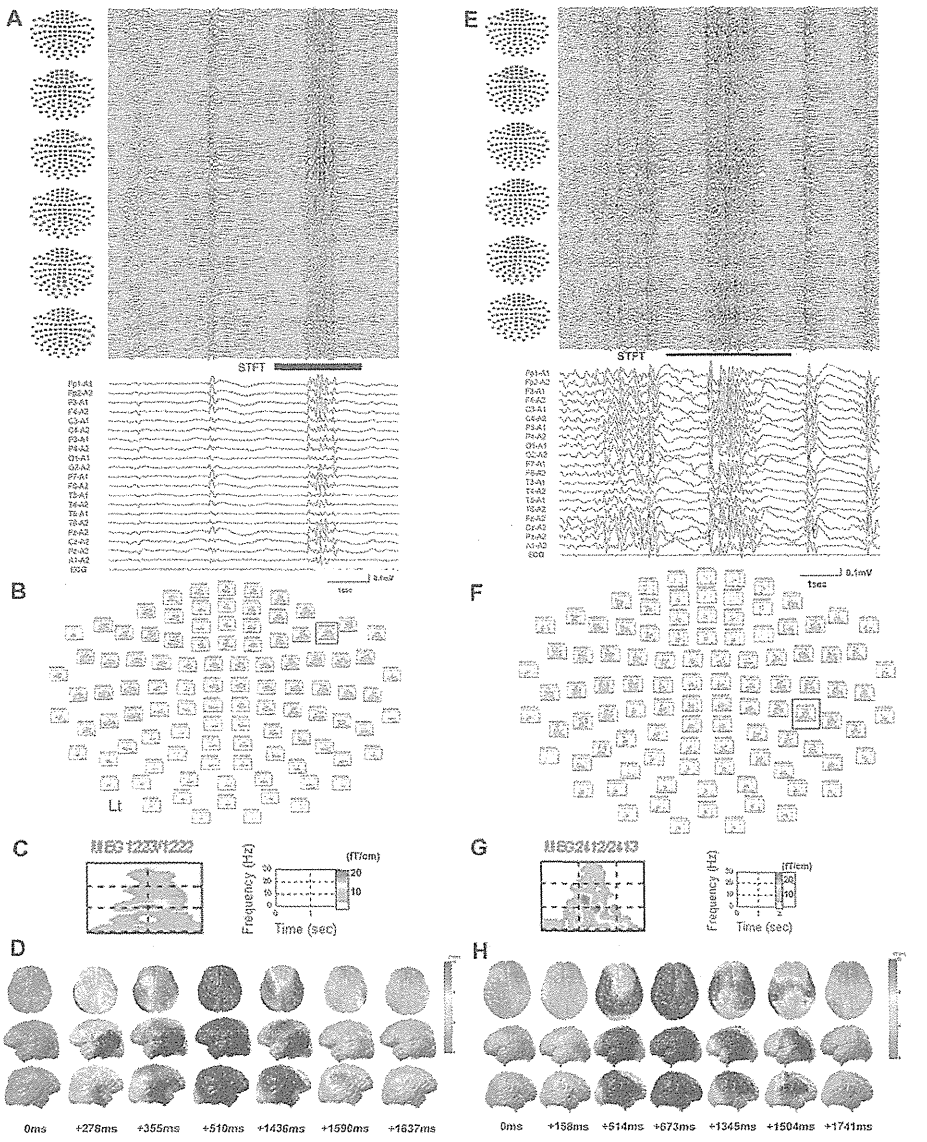

Figure 3 (Patients 4 and 5) Left panel: Patient 4 (A) bottom panel demonstrates diffuse paroxysmal fast activity (PFA) of the electroencephalogram (EEG) and top panel shows the corresponding 204-channel magnetoencephalogram (204ch-MEG). (B) Short-time Fourier transform (STFT) graph of MEG PFA corresponding to the black bar of (A) (C) Power spectrogram of MEG electrode 1223/1222 (black square in STFT graph B) corresponding to the black bar of (A) using STFT to show the wide range of oscillations from 10 to 30 Hz. High-power narrow band oscillations (shown in red) are found at 10 Hz. (D) Superimposed three-dimensional magnetic resonance (3D-MRI) moving image of patient 4 shows oscillations are generated in the bilateral parietal–temporal area and propagated to the whole area. Right panel: Patient 5 (E) Bottom panel demonstrates diffuse PFA of the EEG and top panel shows the corresponding 204ch-MEG. (F) STFT graph of MEG PFA corresponding to the black bar of (E) (G) Power spectrogram of MEG electrode 2412/2413 (black square in STFT graph F) corresponding to the black bar of (E) using STFT to show the wide range of oscillations from 10 to 30 Hz. High-power narrow band oscillations (shown in red) are found at 10–15 Hz. (H) Superimposed 3D-MRI moving image of patient 5 shows oscillations are generated in the bilateral parietal–temporal area and propagated to the whole area.

desynchronization with PFA. This interictal EEG pattern is similar to the ictal EEG pattern of ESs patients (Fusco and Vigevano, 1993; Kellaway et al., 1979). Desynchronization always appears after the clinical spasms and is considered to be a postictal rather than an ictal event (Watanabe et al., 2001).

We successfully recorded an ictal EEG and MEG in Patient 3 and STFT analysis of the ictal MEG showed a focal epileptogenic focus at part of the source of the interictal PFA. Eliashiv et al. (2002) reported that the ictal MEG-defined ictal-onset zone was smaller than the irritative zone defined by interictal MEG and equivalent or superior to invasive

EEG recordings. In our case, the area of ictal MEG specific oscillation was not smaller but overlapped with the area of interictal PFA generation. This result is a good confirmation that analysis of interictal PFA is equivalent to that of ictal fast activity. The specific oscillation of the ictal MEG recording preceded the onset of the clinical seizure, which was confirmed in video monitoring, by several seconds in Patient 3. A similar pattern has been reported in an ictal ECoG study of ESs with focal spike or fast-wave bursts preceding the spasms in a subset of patients with ESs (Asano et al., 2005). They hypothesized that this focal activity may trigger the ESs, leading them to speculate that the cortex may be a trigger of the ESs, and the spasms associated with fast wave bursts may be derived from a cortico-subcorticocortical pathway rather than a cortico-cortical pathway. Our ictal MEG result supports their speculation and the period of no specific oscillation suggests that oscillations were propagating through a subcortical pathway. Moreover, Asano et al. (2001) reported that surgical resection of the focal area can eliminate the spasms. Electrocorticography is effective for the assessment of epileptic activity and to elucidate the ictal-onset zone. However, ECoG is invasive and, it is also difficult to decide on the placement of electrodes especially in non-lesional cases. We have recently reported that MEG fast activity correlates well with ECoG findings, and is therefore useful for presurgical evaluation (Sueda et al., 2010). Our method may be useful for deciding on candidates for epilepsy surgery by predicting the epileptic zone and placement of invasive electrodes.

Advantage over ECD model

The ECD model is based on the assumption that the brain activity generating the signals comprises only a small number of focal sources; therefore the ECD model is not suitable for analyzing cases whose activity seems to be generated from a wide area. Although we attempted to investigate the correlation between ECDs and PFA findings, ECDs were not clustered in Patients 1 and 2, and in Patient 3, ECDs were clustered at the right central–parietal region and the area of ECD and high-power area of MEG PFA were almost concordant. RamachandranNair et al. (2008) reported that all older pediatric patients with ESs had unilateral clusters of MEG spike sources like Patient 3, and a cluster of MEG spike sources represented the epileptogenic zone. However ECD analyses are insufficient to decide the epileptogenic zone in cases like Patients 1 and 2, since the ECD analysis is not suitable for propagated discharges. We consider that STFT analyses of MEG PFA are useful for detecting the epileptogenic zones of patients with ESs.

Comparison between the PFA of LGS and the PFA of ESs

PFA is seen most in patients with LGS hence we analyzed the PFA of LGS to compare with ESs. The STFT analyses and 3D-MRI movie of PFA in LGS showed that PFAs were generated from diffuse whole areas and simultaneously from bilateral hemispheres (Fig. 3). These results suggest that the mechanism of PFA is different between ESs and LGS.

For Patients 1 and 3, PFAs were generated from a focal area on one side of the hemisphere. We could predict the region for localization of epilepsy from the MEG findings and provide a diagnosis of symptomatic localization-related epilepsy, although Patient 1 had been diagnosed with symptomatic generalized epilepsy.

For Patient 2, three of the seven PFAs were generated bilaterally from the frontal areas simultaneously and four PFAs were generated from the right frontal–parietal area and propagated to the left frontal hemisphere. His seizure manifestation quite resembled LGS and his EEG was also described as having a diffuse fast rhythm and slow spike and wave complexes. But our current findings using MEG to examine PFA suggest that his right frontal area is affected dominantly and has an epileptogenic lesion. MEG PFA could be helpful for the precise evaluation of cases like Patient 2.

We considered that the findings in Patient 2 demonstrated the mechanism of secondary bilateral synchrony (SBS). Our STFT method would be useful to differentiate primary bilateral synchrony (PBS) from SBS. Distinguishing PBS from SBS is generally difficult using clinical findings or visual assessment of EEG or MEG data. The minimum transcallosal transferring time is reported as approximately 20 ms (Ono et al., 2002). Therefore, when the interval of the cortico-cortical propagation is longer than 20 ms, it could indicate transcallosal propagation, i.e., SBS. For Patients 1 and 2, the time difference between each hemisphere oscillation in PFA could be estimated as more than 20 ms, meaning SBS. On the contrary, for Patients 4 and 5, no time differences were present, so they had PBS. Although a few studies have shown that MEG can be used to analyze SBS with spike and wave complexes (Smith, 2004; Tanaka et al., 2005) these studies used SDM for their evaluation. As we have mentioned previously, the ECD model is difficult to use for PFA. The SDM analysis can be used for focal discharges, since equivalent dipoles can be calculated by solving the inverse problem with the definition of a single generator. Since STFT can be applied to any activity without the above calculations, our method can be useful for evaluating PBS and SBS.

Limitations

Short-time Fourier transform analysis is limited to patients who have aberrant frequency oscillation like PFA detached from background activity, and cannot reveal the depth of the source, because the planar gradiometers evaluate the magnetic field just beneath the sensor. However, unlike ECD and other spatial filtering methods, STFT can analyze the wide area oscillation and temporal changes without solving the inverse problem for source localization. This point is valuable for STFT analyses.

Conclusion

In conclusion, STFT analyses can show the origin and form of propagation of PFA on MEG. Analyses of MEG PFA using STFT suggest that ESs are one of the representative epileptic seizures of localization-related epilepsy. Analysis of PFA by STFT might be one of the most useful tools to define the classification of epilepsies and epileptic syndromes.

Conflicts of interest

None of the authors has any conflict of interest to disclose.

Acknowledgements

We express our gratitude to Prof. Tadashi Ariga in Department of Pediatrics, Hokkaido University, Graduate School of Medicine, for his valuable editorial opinion.

We confirm that we have read the Journal's position on issues involved in ethical publication and affirm that this report is consistent with those guidelines.

This work was supported in part by Grants-in-aid for Scientific Research (18591136) from the Japan Society of the Promotion of Science, and the Japan Epilepsy Research Foundation.

References

Akiyama, T., Otsubo, H., Ochi, A., Ishiguro, T., Kadokura, G., Ramachandran- Nair, R., Weiss, S.K., Rutka, J.T., Snead III, O.C., 2005. Focal cortical high-frequency oscillations trigger epileptic spasms: Confirmation by digital video subdural EEG. Clin. Neurophysiol. 116, 2819–2825.

Arzimanoglou, A., French, J., Blume, W.T., Cross, J.H., Ernst, J.P., Feucht, M., Genton, P., Guerrini, R., Kluger, G., Pellock, J.M., Perucca, E., Wheless, J.W., 2009. Lennox–Gastaut syndrome: a consensus approach on diagnosis, assessment, management, and trial methodology. Lancet Neurol. 8, 82–93.

Asano, E., Chugani, D.C., Juhasz, C., Muzik, O., Chugani, H.T., 2001. Surgical treatment of West syndrome. Brain Dev. 23, 668–676.

Asano, E., Juhász, C., Shah, A., Muzik, O., Chugani, D.C., Shah, J., Sood, S., Chugani, H.T., 2005. Origin and propagation of epileptic spasms delineated on electrocorticography. Epilepsia 46, 1086–1097.

Berg, A.T., Berkovic, S.F., Brodie, M.J., Buchhalter, J., Cross, J.H., van Emde Boas, W., Engel, J., French, J., Glauser, T.A., Mathern, G.W., Moshé, S.L., Nordli, D., Plouin, P., Scheffer, I.E., 2010. Revised terminology and concepts for organization of seizures and epilepsies: report of the ILAE Commission on Classification and Terminology, 2005–2009. Epilepsia 51, 676–685.

Brenner, R.P., Atkinson, R., 1982. Generalized paroxysmal fast activity: electroencephalographic and clinical features. Ann. Neurol. 11, 386–390.

Chugani, H.T., Rintahaka, P.J., Shewmon, D.A., 1994. Ictal patterns of cerebral glucose utilization in children with epilepsy. Epilepsia 35, 813–822.

Communication on Classification and Terminology of the International League Against Epilepsy, 1989. Proposal for revised classification of epilepsies and epileptic syndromes. Epilepsia 30, 389–399.

Eliashiv, D.S., Elsas, S.M., Squires, K., Fried, I., Engel Jr., J., 2002. Ictal magnetic source imaging as a localizing tool in partial epilepsy. Neurology 59, 1600–1610.

Engel Jr., J., 2006. Report of the ILAE classification core group. Epilepsia 47, 1558–1568.

Feshchenko, V.A., Veselis, R.A., Reinsel, R.A., 1997. Comparison of the EEG effects of midazolam, thiopental, and propofol: the role of underlying oscillatory systems. Neuropsychobiology 35, 211–220.

Feshchenko, V.A., Veselis, R.A., Reinsel, R.A., 2004. Propofol-induced alpha rhythm. Neuropsychobiology 50, 257–266.

Fusco, L., Vigevano, F., 1993. Ictal clinical electroencephalographic findings of spasms in West syndrome. Epilepsia 34, 671–678.

Gobbi, G., Bruno, L., Pini, A., Giovananardi, R.P., Tassinari, C.A., 1987. Periodic spasms: unclassified type of epileptic seizure in childhood. Dev. Med. Child Neurol. 29, 766–775.

Haginoya, K., Munakata, M., Kato, R., Yokoyama, H., Ishizuka, M., Iinuma, K., 2002. Ictal cerebral haemodynamics of childhood epilepsy measured with near-infrared spectrophotometry. Brain 125, 1960–1971.

Kellaway, P., Hrachovy, R.A., Frost Jr., J.D., Zion, T., 1979. Precise characterization and quantification of infantile spasms. Ann. Neurol. 6, 214–218.

Markand, O.N., 2003. Lennox–Gastaut syndrome (childhood epileptic encephalopathy). J. Clin. Neurophysiol. 20, 426–441.

Munakata, M., Haginoya, K., Ishitobi, M., Sakamoto, S., Sato, I., Kitamura, T., Hirose, M., Yokoyama, H., Iinuma, K., 2004. Dynamic cortical activity during spasms in three patients with West syndrome: a multichannel near-infrared spectroscopic topography study. Epilepsia 45, 1248–1257.

Ohtsuka, Y., Kobayashi, K., Ogino, T., Oka, E., 2001. Spasms in clusters in epilepsies other than typical West syndrome. Brain Dev. 23, 473–481.

Ono, T., Matsuo, A., Baba, H., Ono, K., 2002. Is a cortical spike discharge "transferred" to the contralateral cortex via the corpus callosum?: an intraoperative observation of electrocorticogram and callosal compound action potentials. Epilepsia 43, 1536–1542.

Oppenheim, A., Schafer, R.W., 1999. Discrete-Time Signal Processing. Prentice Hall, NJ.

Panzica, F., Franceschetti, S., Binelli, S., Canafoglia, L., Granata, T., Avanzini, G., 1999. Spectral properties of EEG fast activity ictal discharges associated with infantile spasms. Clin. Neurophysiol. 110, 593–603.

RamachandranNair, R., Ochi, A., Imai, K., Benifla, M., Akiyama, T., Holowka, S., Rutka, J.T., Snead 3rd, O.C., Otsubo, H., 2008. Epileptic spasms in older pediatric patients: MEG and ictal high-frequency oscillations suggest focal-onset seizures in a subset of epileptic spasms. Epilepsy Res. 78, 216–224.

Smith, M.C., 2004. The utility of magnetoencephalography in the evaluation of secondary bilateral synchrony: a case report. Epilepsia 45 (Suppl. 4), 57–60.

Sueda, K., Takeuchi, F., Shiraishi, H., Nakane, S., Asahina, N., Kohsaka, S., Nakama, H., Otsuki, T., Sawamura, Y., Saitoh, S., 2010. MEG time-analyses for pre and post surgical evaluation of patients with epileptic rhythmic fast activity. Epilepsy Res. 88, 100–107.

Tanaka, N., Kamada, K., Takeuchi, F., Takeda, Y., 2005. Magnetoencephalographic analysis of secondary bilateral synchrony. J. Neuroimaging 15, 89–91.

Watanabe, K., Negoro, T., Okumura, A., 2001. Symptomatology of infantile spasms. Brain Dev. 23, 453–466.

Original article

Epileptic Disord 2012; 14 (1): 32-40

Clinical patterns and pathophysiology of hypermotor seizures: an ictal SPECT study

Hiroshi Masuda [1], Erum Shariff [1], John Tohyama [2], Hiroatsu Murakami [1], Shigeki Kameyama [1]

[1] Department of Neurosurgery
[2] Department of Pediatrics, Nishi-Niigata Chuo National Hospital, Niigata, Japan

Received June 11, 2011; Accepted December 21, 2011

ABSTRACT – Hypermotor seizures (HMS) can include different forms of hypermotor behaviour due to various mechanisms associated with generation of ictal automatisms. Despite the varied location of seizure onset, similar semiologic features during seizures may exist. Ictal single-photon emission tomography (SPECT) apparently reflects not only the origin of epileptic discharge but also the spread to adjacent cortical areas. Taking this benefit of SPECT studies into account, preoperative SPECT results from 13 patients with HMS who underwent epilepsy surgery were analysed. The radioisotope 99mTc-ECD was injected in all patients within five seconds after seizure onset. Group analysis was performed with statistical parametric mapping (SPM) of paired ictal-interictal SPECTs in order to identify regions of significant ictal hyperperfusion. Hyperperfused regions with a corrected cluster-level significance p-value of < 0.002 were considered significant. Seizure onset at implanted subdural electrodes was defined as the epileptic focus in 12 of 13 patients. Two patterns were recognized: HMS-1 with marked agitation and HMS-2 with mild agitation. Ictal hyperperfusion images revealed significant hyperperfusion in the anterior cingulate cortex, orbito-frontal gyrus, lentiform nucleus, midbrain and pons. These hyperperfused areas represent the symptomatogenic zone which was different from the epileptogenic zone, as confirmed by the favourable outcomes after surgical resection. The present findings suggest that a network, including frontal and possibly extrafrontal brainstem and limbic structures, is involved in the genesis of the complex epileptic manifestations of HMS. Moreover, ictal SPECT analysed by SPM is a useful method for studying the neural networks of different types of seizures.

Key words: anterior cingulate cortex, frontal lobe epilepsy, hypermotor seizures, statistical parametric mapping (SPM), symptomatogenic zone

Correspondence:
Erum Mubbashar Shariff
Department of Functional Neurosurgery,
Epilepsy Centre
Nishi-Niigata Chuo National Hospital,
1-14-1 Masago, Nishi-ku,
Niigata City, Niigata 950-2085, Japan
<drerumshariff@hotmail.com>

doi:10.1684/epd.2012.0485

Analysis of seizure semiology is an important element of presurgical evaluation and is often used to distinguish temporal versus frontal onset (Holthausen and Hoppe, 2000). Because the clinical features of seizures are produced from activation of certain regions of the brain and spread to certain areas, detailed analysis of ictal semiology can often provide insights into the lateralising information of seizure focus and seizure propagation pathways (Chee *et al.*, 1993; Kotagal *et al.*, 1995; Marks and Laxer, 1998). Intracranial electrodes can provide a more precise localisation of seizure focus (Shin *et al.*, 2002) and are often necessary for localisation of the epileptogenic zone (EZ). However, they record only a small portion of the brain, therefore, electrode placement requires guidance by other evidence. The role of ictal SPECT for localisation of the ictal onset zone has already been established (Knowlton *et al.*, 2004; Lee *et al.*, 2005). SPECT has the unique advantage of mapping brain activity at the time of radiotracer injection (during a seizure) and the actual imaging can be performed up to 60-90 minutes later, when the patient is fully stable (McNally *et al.*, 2005). Even though it is used primarily in the presurgical evaluation of refractory patients to localise the ictal onset zone, ictal SPECT also shows hyperaemic regions which represent propagated ictal activity, because radiopharmaceutical is injected after noting seizure onset (Van Paesschen *et al.*, 2007). Therefore, ictal hyperperfusion topography should reflect activated structures responsible for the evolution of symptomatology during the seizure course.

Hypermotor seizures (HMS) have been studied extensively for identification of the epileptogenic zone (EZ), but studies regarding the symptomatogenic zone responsible for the hypermotor activity are sparse (Wong *et al.*, 2010). Using ictal SPECT and voxel-based analysis, the aim of the present study was to identify the neuronal networks generating specific ictal symptomatology in patients with HMS.

Methods

Patient selection and clinical characteristics

A retrospective analysis was conducted with patients selected from a database of 291 patients who had undergone an operation for refractory partial epilepsy at our institution between 1996 and 2008. A total of 13 patients were identified with HMS. HMS was defined as ictal complex motor agitation with proximal movements of the limbs, including body rocking, kicking or boxing movements, and horizontal or rotatory movements of the trunk and pelvis while lying on a bed (Williamson *et al.*, 1985; Waterman *et al.*, 1987; Lüders *et al.*, 1998; Blume *et al.*, 2001). Inclusion and exclusion criteria were chosen to identify a homogeneous group of patients with HMS. Consecutive patients meeting the following inclusion criteria were included: (a) refractory epilepsy with HMS as the only seizure type; (b) early ictal SPECT injection (defined as being given <5 seconds after the start of a clinical or electrographic seizure or within the first half of a seizure) and ongoing seizure activity monitored under video-EEG during an episode of HMS; (c) interictal SPECT after a seizure-free period of at least 24 hours; and (d) post-surgery follow-up of at least two years. Exclusion criteria were as follows: (a) patients with mixed-type complex partial seizures (CPS) and (b) ictal injection during the postictal state or after the first half of a seizure. A diagnosis of HMS was made based on history obtained from the relatives and review of the video-EEG tapes by three of the authors. These three authors also visually assessed the SPECT findings and reviewed the findings of subtraction ictal SPECT co-registered to MRI (SISCOM) and SPM.

The following aspects were obtained from all patients: clinical characteristics (age at epilepsy surgery, sex, age at seizure onset, epilepsy duration, family history of epilepsy and history of febrile seizures), follow-up period after surgery, surgical outcome, and seizure semiology at the time of the ictal SPECT study.

Seizure evaluation

The video tapes of all recorded seizures for each patient were reviewed. Three of the authors independently analysed clinical semiology. In the case of differing conclusions among the three investigators, consensus was achieved by common re-analysis of seizures. A total of 120 seizures were recorded in the 13 patients. All patients had HMS. The main ictal manifestations were categorised according to the International League Against Epilepsy (ILAE) classification (Blume *et al.*, 2001) and Rheims' classification (Rheims *et al.*, 2008). They were listed as follows: (1) groaning or shouting; (2) asymmetric tonic or dystonic posturing; (3) bilateral tonic or dystonic posturing; (4) marked agitation including body rocking, kicking or boxing behaviour associated with sitting up; and (5) mild agitation characterised by horizontal movements or rotation of trunk and pelvis.

SPECT and MRI techniques

Interictal SPECT studies were performed by injection of 99mTc-ethyl cysteinate dimer (ECD) under intravenous sedation with midazolam. Midazolam was only given to patients with frequent seizures (two patients with less frequent seizures were excluded; Cases 12

and 13, who had four seizures in a month). Ictal SPECT studies were performed by intravenous injection of 99mTc-ECD. The injection line was flushed thoroughly with saline immediately after seizure onset by personnel well acquainted with the patient's seizures and who were stationed at the bedside. The time of seizure onset was defined as the time of the earliest abnormal movements or behaviour, or the onset of impaired awareness or electrographic changes, whichever came first. The interval between seizure onset and time of injection was no more than five seconds. The administered dose was 600 MBq for adult patients and was determined using a formula [600 × (body weight in kg/60) 2/3] MBq for paediatric patients. SPECT imaging was performed by two head cameras (Picker Prism 2000XP, Picker International Inc., Uniontown, OH, USA). The data were acquired in 128×128 matrices over 20-minute periods. A total of 128 brain slices were obtained by T1-weighted MRI sequences (3D/SMASH, 1.5 Tesla, Shimadzu, Kyoto, Japan) (repetition time: 9.76 milliseconds; echo time: 4.4 milliseconds; flip angle: 15 degrees; matrix: 256×256; field of view: 260×260; width: 1.3 mm; gapless). Reconstructed images were reoriented to axial, sagittal, and coronal slices.

SPM Study

SPECT analysis was performed using SPM software (version SPM2, Wellcome Department of Cognitive Neurology, London, UK) and was run on a MATLAB 6.1 (The Mathworks, Inc., Natick, MA, USA) platform. Default SPM2 parameters for analysis of SPECT images were used, except where noted. Before analysis, SPECT images of the patients with ictal onset arising from the left side were flipped onto the right side to allow group analysis of ipsilateral and contralateral perfusion changes. For paired ictal-interictal comparisons, interictal SPECT images of each patient were linearly transformed to match the ictal SPECT image. Ictal SPECT images were spatially normalised to the standard SPECT template using a 12-parameter affine and a further non-linear transformation, and the transformation matrix of the ictal SPECT was subsequently adjusted to the interictal SPECT of the same patient. Spatially normalised images were then smoothed using an isotropic Gaussian kernel with a 12-mm full width at half maximum (FWHM) to increase the signal-to-noise ratio. A height threshold (individual voxel-level significance) was set at p-value <0.002. The extent threshold was set to KE = 125. The coordinates of cluster peak were determined using "Automated Talairach Atlas labels for functional brain mapping" (Lancaster *et al.*, 2000). The results were displayed on the three-dimensional planes of a standard T1-MRI template.

Electrocorticographic records

In 12 of 13 patients, a variable degree of inconsistency was observed among the anatomo-electro-clinical data as to the localisation of the epileptogenic zone (EZ), indicating the need for an ECoG investigation. For each patient, one recorded seizure was selected which was the same type as, and typical of, the seizure studied during ictal SPECT. Based on this epileptic discharge, sites of onset and propagation were determined. All patients had a post-operative follow-up of at least 36 months (36-144 months).

All but one patient (Case 2) underwent ECoG monitoring. Since one patient (Case 1) underwent two ECoGs, owing to continuing seizures after the first ECoG-based, left frontal FCD resection, 13 procedures were performed. Investigations were right-sided in six patients, left-sided in five patients and bilateral in one patient (Case 6). Inter-hemispheric electrodes were placed in five patients. Additional depth electrodes were placed in three patients.

Results

Demographic and other key aspects of the study population are summarised in *table 1*. There were 13 patients: 10 male and three female. Age at presentation was 3-58 years, with a mean age of 23.7 years. The age at operation ranged from 9 to 58 years with a mean age of 26.8 years.

All HMS behaviour resulted in complex agitation; however, the intensity of agitation varied among patients, allowing differentiation of two types of HMS, as suggested by Rheims *et al.* (2008). Vocalisations of shouting and groaning, dystonic posturing, and change in facial expressions were accompanying symptoms. A detailed seizure description is presented in *table 2*.

SPECT image analysis: visual and SISCOM

Analysis of SPECT images was performed by visual side-by-side analysis using SISCOM and SPM.

For visual analysis, the EZ was correctly localised by ictal SPECT in only five patients (two with FLE [frontal lobe epilepsy] and three with TLE [temporal lobe epilepsy]). In three patients, there were bilateral increased perfusion areas (IPAs) over the frontal lobe, which were more prominent ipsilateral to the lesion. In five patients, SPECT showed midline IPAs with ACC (anterior cingulate cortex) involvement (four with FLE and one with TLE), while in two patients no IPAs were identified on ictal SPECT (both with FLE; Cases 5 and 10).

Interictal SPECT was normal in five patients, showed hypoperfusion of the EZ in five patients (two with FLE

Table 1. Patient characteristics.

	Sex	Age at onset (yr)	Age at presentation (yr)	Age at operation (yr)	Duration of epilepsy (yr)	Seizure frequency (times/month)	Epilepsy type	Lesion type	Pathological findings	Outcome (Engel)	Follow-up (months)
1	M	2.3	3	9	6.8	500	FLE	FCD	FCD	I	163
2	M	13	28	33	20	100	FLE	FCD	FCD	I	154
3	F	2	24	24	22	30	FLE	Non-lesional	none	III	112
4	M	10	23	24	14	100	FLE	tuberous sclerosis	TS	I	98
5	M	12	31	34	22	500	FLE	FCD	FCD	I	99
6	M	8	18	18	10	30	FLE	Non-lesional	FCD	I	78
7	M	6	12	20	14	30	FLE	Non-lesional	FCD	III	64
8	F	4	19	20	16	30	FLE	FCD	FCD	I	60
9	M	3	21	28	25	30	FLE	Non-lesional	FCD	I	39
10	F	9	58	58	45	30	FLE	FCD	FCD	I	44
11	M	2.7	11	13	10.3	30	TLE	Non-lesional	FCD	I	38
12	M	2	24	27	25	4	TLE	Non-lesional	none	I	51
13	M	13	36	38	25	4	TLE	Non-lesional	FCD	III	39

FLE: frontal lobe epilepsy; TLE: temporal lobe epilepsy; FCD: focal cortical dysplasia; TS: tuberous sclerosis; yr: year.

and three with TLE), showed bilateral frontal hypoperfusion in one patient with right FLE (Case 4), and showed midline hyperperfusion in two patients (both with FLE).

The EZ was correctly localised by SISCOM in 10 patients; detailed findings are presented in *table 3*.

SPM analysis

Ictal hyperperfusion images in the SPM group analysis of paired ictal-interictal SPECTs of 13 patients revealed significant hyperperfusion in the ACC, orbitofrontal gyrus (OFG), lentiform nucleus (LFN) and midbrain. *Figure 1* shows the mapped areas of statistically significant increases in blood flow as a fusion image with maximal intensities at the OFG at a t-value of 7.38 at SPM coordinates (x, y, z), (mm) equal (14, 32, -28), and at the right ACC at a t-value of 4.65 with coordinates 8, 28, 18 on the sagittal, coronal, and axial sections, respectively. Other statistically significant areas of increased regional cerebral blood flow (rCBF) obtained were the LFN at a t-value of 4.19 (22, 4, 0), the claustrum at a t-value of 4.80 (26, 20, 8), the midbrain at a t-value of 4.69 (2, -22, -6), and the pons at a t-value of 4.79 (4, -16, -30).

SPM analysis was also performed on each group of patients, which did not reveal any significant results at $p<0.002$. Analysis was then performed at $p<0.003$, which revealed hyperperfusion in the white matter, the closest grey matter in the left frontal lobe, the subcallosal gyrus, Brodmann area 25 in HMS-2, and the right brainstem including the medulla in HMS-1 (*figure 2*).

Electrocorticography

Subdural electrodes were placed in all patients and additional depth electrodes were placed in three patients. Detailed ECoG findings are presented in *table 3*. The ictal onset zone included the lateral frontal cortex in nine patients, anterior temporal cortex in two patients, parieto-temporal cortex in one patient and the ACC in one patient.

Surgery and outcome

All 13 patients underwent epilepsy surgery. Surgery involved resection of the frontal lobe in nine patients, the temporal lobe in three patients and the left ACC in one patient. The EZ localised by focal low-amplitude fast activities or rhythmic spikes on a few electrodes